Supporting Information

Kucukdereli et al. 10.1073/pnas.1104977108

SI Materials and Methods

Step-by-step protocols for all procedures are available upon request from the corresponding author.

Purification and Primary Culture of RGCs and Astrocytes. RGCs were purified by sequential immunopanning to greater than 99.5% purity from P5 Sprague–Dawley rats (Charles River) and cultured in serum-free medium containing BDNF, CNTF, and forskolin on laminin-coated coverslips, as previously described (1–3). Cortical astrocyte inserts and ACM were prepared as described previously (1). RGCs were cultured for 3 to 4 d to allow robust process outgrowth and subsequently cultured with astrocyte inserts, ACM, hevin, SPARC, SLF, or TSP for an additional 6 d.

Recombinant Proteins and DNA Constructs. Full-length hevin cDNA as well as its truncation construct SLF were cloned into pAPtag5 vector (GeneHunter) between SfiI and XhoI sites. Hevin constructs were expressed by HEK293 cells, which were transfected by using Lipofectamine 2000 (Invitrogen) according to the manufacturer's instructions. The secreted recombinant proteins were purified from conditioned culture media by Ni-chelating chromatography using Ni-NTA resin (Qiagen) according to the manufacturer's instructions. Purified human platelet TSP1 was obtained from Haematologic Technologies. Purified full-length SPARC was prepared as described previously (4).

Synapse Assay on RGCs. For synapse quantification of RGC cultures, cells were fixed for 7 min with 4% paraformaldehyde (PFA), washed three times in PBS solution, and blocked in 100 μL of a blocking buffer containing 50% normal goat serum and 0.1% Triton X-100 for 30 min. After blocking, coverslips were washed three times in PBS solution, and 100 μL of primary antibody solution was added to each coverslip, consisting of rabbit anti-synaptotagmin (1:750; cytosolic domain; Synaptic Systems) and mouse anti-PSD95 (1:750; 6G6-1C9 clone; Affinity BioReagents). In some experiments, presynaptic antibody against bassoon (1:500; Stressgen) and postsynaptic antibody against all isoforms of homer (1:1,000; Chemicon) were used. Coverslips were incubated overnight at 4 °C, washed three times in PBS solution, and incubated with 100 μL of Alexa-conjugated secondary antibodies (Invitrogen) diluted 1:1,000 in antibody buffer. Following incubation for 2 h, coverslips were washed three or four times in PBS solution and mounted in Vectashield mounting medium with DAPI (Vector Laboratories) on glass slides (VWR Scientific). Secondary-only controls were routinely performed and revealed no significant background staining.

Mounted coverslips were imaged on an Eclipse E800 epifluorescence microscope (Nikon). Healthy cells that were at least two cell diameters from their nearest neighbor were identified and selected at random by eye by DAPI fluorescence. Eight-bit digital images of the fluorescence emission at 594 nm and 488 nm were recorded for each selected cell using a monochrome CCD camera and SPOT image capture software (Diagnostic Instruments). Merged images were analyzed for colocalized puncta with a custom plug-in (written by Barry Wark; available upon request from c.eroglu@cellbio.duke.edu) for the NIH image-processing package ImageJ. The details of this quantification method can be found in a previous publication (5). This synapse number analysis technique has been verified numerous times to generate counts that are similar to the numbers we obtain counting by eye. We have previously shown that this increase in colocalized puncta corresponds to a real increase in the number of synapses, which were counted by EM and confirmed by electrophysiological analysis (1, 3).

Electrophysiology. mEPSCs were recorded by whole-cell patch-clamping RGCs at room temperature (18 °C–22 °C) at a holding potential of −70 mV. The extracellular solution contained (in mM) 140 NaCl, 2.5 $CaCl_2$, 2 $MgCl_2$, 2.5 KCl, 10 glucose, 1 NaH_2PO_4 and 10 Hepes (pH 7.4), plus TTX (1 μM) to isolate mEPSCs. Patch pipettes were 3 to 5 MΩ, and the internal solution contained (in mM) 120 K-gluconate, 10 KCl, 10 EGTA, and 10 Hepes (pH 7.2). mEPSCs were recorded using pClamp software for Windows (Axon Instruments), and were analyzed with Mini Analysis Program (SynaptoSoft).

EM. RGCs were fixed for EM in 4% glutaraldehyde in PBS solution as previously described (1, 3) and viewed with a Philips Electronic Instruments CM-12 transmission electron microscope. Synapses were counted by eye under the electron microscope by finding a cell body and dendrites and counting all synapses within a circular field of radius approximately one cell body diameter.

For EM analysis of the mouse SCs, three P25 hevin-null mice on a 129/Sve background and three age-matched WT controls were first transcardially perfused with warm PBS solution to clear out blood cells, and then with warm (37 °C) 2% PFA, 2.5% glutaraldehyde, 2 mM $CaCl_2$, and 4 mM $MgCl_2$ in 0.1 M cacodylate buffer (pH 7.4) under anesthesia. SCs were removed and sliced coronally. SC slices were immersed in 2% glutaraldehyde, 2 mM $CaCl_2$, and 4 mM $MgCl_2$ in 0.1 M cacodylate buffer (pH 7.4) and fixed overnight at 4 °C. Slices were rinsed in 0.1 M cacodylate buffer and postfixed in 1% OsO_4 for 2 h after heating in a microwave (1 min on, 1 min off, then 1 min on). After rinsing with veronal acetate buffer, they were incubated in 2% uranyl acetate for 1.5 h. After a second rinse with veronal acetate, the slices were dehydrated in ethanol series enhanced with 40 s of microwave processing and soaked in propylene oxide. They were next incubated in 50:50 (propylene oxide:epon resin) overnight at room temperature after microwave treatment for 3 min. The slices were then embedded following resin exchange (3×) in 100% epon resin for 2 h. Ultrathin sections were cut and were stained with uranyl acetate and lead citrate.

Sections were viewed under a Philips Electronic Instruments CM-12 transmission electron microscope. Individual neuronal cell bodies were picked within the area of 50 to 150 μm under the pia corresponding to the target zone of RGCs. High-magnification (13,000×) consecutive images were taken in a diameter of 20 μm around the cell body. These images were then tiled together by using the Photomerge algorithm in the Photoshop software package (Adobe). Resolution of high-magnification images was conserved during the tiling process. Synapses were counted and their morphological parameters were analyzed by hand by ImageJ software (NIH) from the composite tiled images.

Immunodepletions, Immunoprecipitation, and Western Blotting. Hevin and SPARC immunodepletions were carried out as follows: astrocytes were grown until confluent in 10-cm tissue culture dishes. Cells were washed three times with warm Dulbecco PBS solution to remove serum. Ten milliliters per plate RGC growth media without B27, BDNF, CNTF, and forskolin was added to each plate, and the medium was conditioned for an additional 6 d. Cleared ACM was concentrated 10 times by centrifugal concentrators (5-kDa cutoff; Sartorius). The 10× ACM was incubated for 3 h with Protein A/G agarose beads (Pierce) that

were prebound to rabbit polyclonal antibodies developed in the laboratory against hevin or SPARC or preimmune rabbit sera overnight. The ACM was cleared of the beads and was transferred into a new tube. Three rounds of depletion were necessary to remove all hevin from ACM. To monitor removal of hevin or SPARC, the beads were washed four or five times and the bound proteins were eluted in 2× SDS/PAGE loading buffer (Pierce).

For hevin–SPARC immunoprecipitation, 1 μg/mL of hevin or SPARC or hevin and SPARC together were precleared with Protein A/G agarose beads (Pierce) in 0.2% BSA in PBS solution with Tween (0.2%). One milliliter from each condition was mixed with 3 μg of mouse anti-Myc antibody (Millipore) and incubated for 1 h at 4 °C. Proteins were resolved by SDS/PAGE on Mini-Protean TGX 4% to 15% gradient gels (Bio-Rad). Hevin and SPARC were detected on Western blots with goat anti-hevin or anti-SPARC antibodies (R&D Systems).

WT mice (129/Sve background) were purchased from Charles River Laboratories. WT mice of different ages (n = 4–5 mice per age) were perfused with PBS solution to clear out blood cells, and the brains were removed. SCs were carefully dissected and homogenized in ice-cold M-PER solution (Pierce) containing protease inhibitors (Roche). The homogenates were cleared of cell debris and insoluble materials by centrifugation at 20,000 × g. The protein concentrations in the lysates were determined by Micro BCA protein assay kit (Pierce). Samples for SDS/PAGE were prepared at 1 μg/μL concentration by using 2× Laemmli sample buffer (Bio-Rad) or 5× SDS/PAGE buffer (Pierce). Fifteen micrograms of protein was loaded into each well. Samples were resolved by SDS/PAGE on 7.5% or 10% polyacrylamide gels and electrophoretically transferred onto nitrocellulose membranes by using Trans-Blot semidry transfer cell (Bio-Rad).

Blots were incubated in primary antibody dilutions in 2% BSA and 0.2% Tween-20 in PBS solution for 2 h after blocking in 10% dry milk in PBS solution with Tween-20 (0.1%, Promega) for 1 h at room temperature. Hevin was detected in Western blots by a rat monoclonal antibody, clone name 12:155 (6), or by goat anti-hevin polyclonal antibodies (0.1 μg/mL; R&D Systems). SPARC was detected in the Western blots by goat anti-SPARC polyclonal antibodies (0.1 μg/mL; R&D Systems). Horseradish peroxidase-conjugated anti-rat or anti-goat (1:5,000) IgGs were used as secondary antibodies (Jackson Laboratories), and the detection was performed with an ECL kit (GE) or Super Signal West Femto detection kit (Pierce).

Hevin and SPARC IHC. WT (129/Sve) mice of different ages were perfused with PBS solution to clear out the blood. Brains were immersed in 4% PFA, fixed overnight at 4 °C, and cryoprotected in 30% sucrose. Tissue was embedded in a 2:1 mixture of 20% sucrose in PBS:optimum cutting temperature compound and cryosectioned (12 μm). Freshly cut sections were dried at 37 °C and washed three times in PBS solution. For hevin staining, sections were blocked with 50% normal goat serum (NGS; Invitrogen) with 0.5% Triton X-100 (Roche) in PBS solution for 1 h. Rat anti-hevin monoclonal antibody 12:155 was diluted in PBS solution with 0.2% Triton X-100 and 10% NGS at a final concentration of 1 μg/mL. For SPARC and nestin stainings and hevin/SPARC costaining, sections were permeabilized with 0.3% Triton X-100 in PBS solution for 30 min and blocked with donkey serum (4% in PBS solution) for 30 min. These sections were stained with goat anti-SPARC polyclonal antibody (R&D Systems) and/or rat anti-hevin monoclonal antibody 12:155 (1 μg/mL), and rabbit anti-nestin (1:1,000; Covance) diluted in PBS solution with 2% donkey serum by incubation overnight at 4 °C. Secondary Alexa-conjugated antibodies (donkey anti-goat Alexa 488, donkey anti-rat 488, or donkey anti-rabbit 594; Invitrogen) were added (1:200 in the same buffer as the primary antibodies) for 2 h at room temperature in the dark. Slides were mounted in Vectashield with DAPI and were imaged on a Leica SP5 confocal laser-scanning microscope. Confocal scans (5 μm) of the outer layer of the SCs were performed (optical section width, 0.33 μm; 15 optical sections each) at 40× magnification. The scanning parameters were set for the age that has the highest expression (P15 for hevin and SPARC).

Synapse Quantification in Mouse Brain Sections. Hevin- or SPARC-null mice (7, 8) and age- and background-matched WT controls were used for IHC-based synapse number analysis (n = 3–4 mice per age per genotype). Brains were immersed in 4% PFA, fixed overnight at 4 °C, and cryoprotected in 30% sucrose. For synaptic staining, tissue was embedded in a 2:1 mixture of 20% sucrose:optimum cutting temperature compound in PBS solution and cryosectioned (12 μm). Sections were dried at 37 °C, washed one time in PBS solution, and blocked with 20% NGS (Invitrogen) in PBS solution for 1 h. Primary antibodies were diluted in PBS solution with 0.3% Triton X-100 and 10% NGS as follows: PSD95 (rabbit, 1:500; Zymed) and VGlut2 (guinea pig, 1:2,500; Chemicon) and incubated overnight at 4 °C. Secondary Alexa-conjugated antibodies (goat anti-guinea pig Alexa 488 and goat anti-rabbit Alexa 594; Invitrogen) were added at 1:500 in the same buffer for 2 h at room temperature in the dark. Slides were mounted in Vectashield with DAPI and were imaged on a Leica SP5 confocal laser-scanning microscope.

Three independent sagittal brain sections per animal were stained with pre- and postsynaptic markers, and 5-μm confocal scans were performed (optical section width, 0.33 μm; 15 optical sections each) at 63× magnification. To ensure consistency of the area to be scanned, we chose the outer SC region adjacent to the inferior colliculus, encompassing the synaptic layer for retinocollicular terminals in each section. We imaged and quantified the synapses in the upper 150-μm synaptic zone of the SC, where RGC axons are known to establish contacts. The parameters for scanning were established for WT brain sections, and the same imaging parameters were used for hevin-null animals. In experiments to determine synapse number in SPARC-null mice, the parameters for scanning were established for SPARC-null brain sections, and the same imaging parameters were used for WT animals. Maximum projections of three consecutive optical sections corresponding to 1-μm sections were analyzed by using the ImageJ puncta analyzer option to count for number of colocalized pre- and postsynaptic puncta (≥5 optical sections per brain section and ≥15 total images per brain). Average synaptic density per imaged area was calculated for each condition.

Golgi–Cox Staining and Dendritic Morphology Analysis. Golgi–Cox staining was performed on hevin-null and age-matched WT control mice (n = 3 mice per genotype) as described in the FD Rapid GolgiStain Kit (FD NeuroTechnologies). Dye-impregnated brains were embedded in Tissue Freezing Medium (Tris-buffered saline solution) and were rapidly frozen on ethanol pretreated with dry ice. Brains were cryosectioned sagittally at 80 μm thickness and mounted on gelatin-coated microscope slides (Southern Biotech). Sections were stained according to the directions provided by the manufacturer. RGC target neurons in the SC were analyzed for their morphology. RGC target neurons in the upper and lower SGS were divided into WFII or stellate neurons based on morphology (9, 10). WFII and stellate neurons from three brains of each genotype (n = 22 neurons total per cell type) were traced by the use of Neurolucida software (MBF Bioscience). The dendritic trees of each neuron were determined for area and perimeter by convex hull analysis, and the complexity of the dendritic tree was calculated by Sholl analysis. All analyses were performed by NeuroExplorer (MBF Bioscience).

Axonal Innervation Analysis. P3 hevin-null and WT control mice were given unilateral cholera toxin-β subunit conjugated to Alexa 594 (CTβ) injection into their right eyes. Axonal innervation area was analyzed from the CTβ-labeled area in the SC contralateral

to the side of the injected retina. Fluorescence microscopic images were analyzed by using the Li minimum cross entropy method, and the area of CTβ-labeled axons was automatically quantified with ImageJ software (NIH).

1. Christopherson KS, et al. (2005) Thrombospondins are astrocyte-secreted proteins that promote CNS synaptogenesis. *Cell* 120:421–433.
2. Meyer-Franke A, Kaplan MR, Pfrieger FW, Barres BA (1995) Characterization of the signaling interactions that promote the survival and growth of developing retinal ganglion cells in culture. *Neuron* 15:805–819.
3. Ullian EM, Sapperstein SK, Christopherson KS, Barres BA (2001) Control of synapse number by glia. *Science* 291:657–661.
4. Sage EH (2003) Purification of SPARC/osteonectin. *Curr Protoc Cell Biol* 10:11.1–11.23.
5. Ippolito DM, Eroglu C (2010) Quantifying synapses: An immunocytochemistry-based assay to quantify synapse number. *J Vis Exp* 45:pii2270.
6. Brekken RA, et al. (2004) Expression and characterization of murine hevin (SC1), a member of the SPARC family of matricellular proteins. *J Histochem Cytochem* 52: 735–748.
7. Barker TH, et al. (2005) Matricellular homologs in the foreign body response: Hevin suppresses inflammation, but hevin and SPARC together diminish angiogenesis. *Am J Pathol* 166:923–933.
8. Sullivan MM, et al. (2006) Matricellular hevin regulates decorin production and collagen assembly. *J Biol Chem* 281:27621–27632.
9. Ogawa T, Takahashi Y (1981) Retinotectal connections within the superficial layers of the cat's superior colliculus. *Brain Res* 217:1–11.
10. Warton SS, Jones DG (1985) Postnatal development of the superficial layers in the rat superior colliculus: A study with Golgi-Cox and Klüver-Barrera techniques. *Exp Brain Res* 58:490–502.

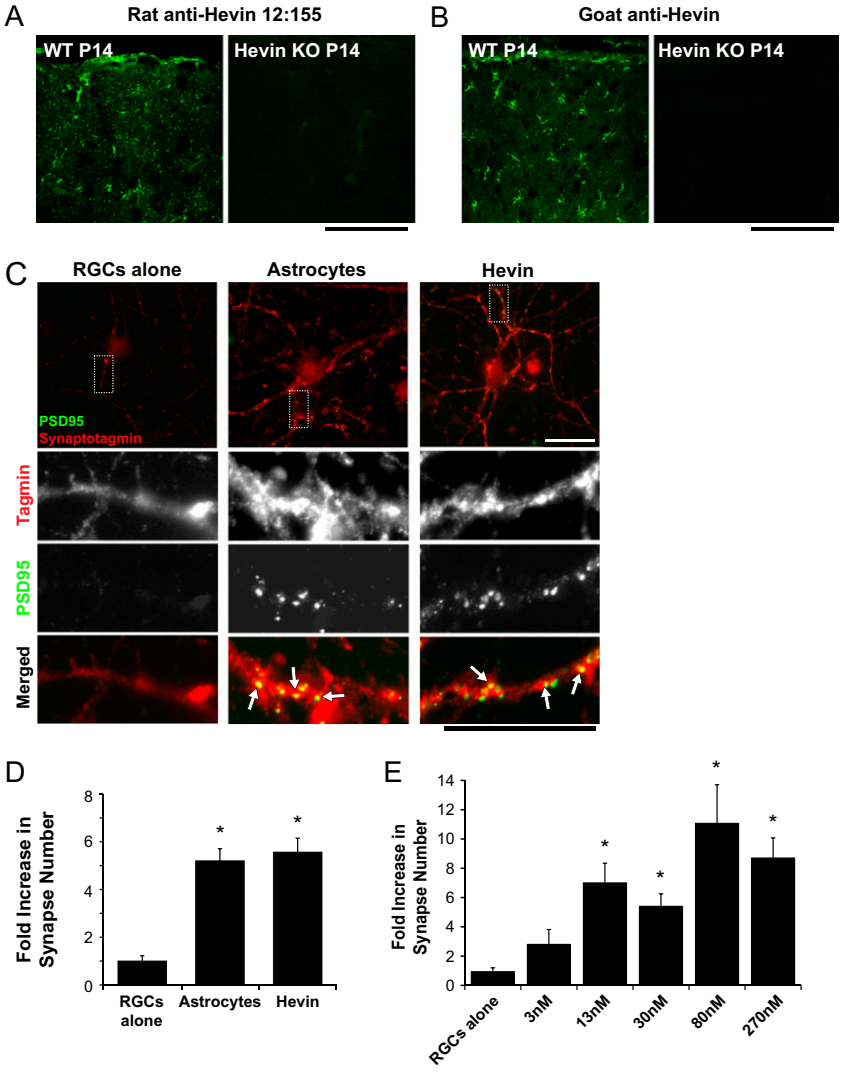

Fig. S1. Hevin is expressed by astrocytes and induces synapse formation on RGCs in culture. Immunostaining of SCs from sagittal brain sections of P14 WT and hevin-null (Hevin-KO) mice with (*A*) rat anti-hevin monoclonal antibody (clone 12:155) or (*B*) goat anti-hevin polyclonal antibody (R&D Systems). Neither 12:155 antibody nor goat anti-hevin polyclonal antibody stained KO brains, showing that these antibodies are highly specific for hevin. (Scale bar: 100 μm.) (*C*) Immunostaining of RGCs for colocalization of presynaptic vesicular marker synaptotagmin (red) and PSD marker PSD95 (green) showed few colocalized synaptic puncta in the absence of astrocytes but many in the presence of a feeding layer of astrocytes (*Middle*) or 30 nM recombinant hevin (*Right*). Higher-magnification images are marked with white arrows to demonstrate synaptic puncta. (Scale bars: 30 μm.) (*D*) Quantification of the effects of astrocytes or hevin on the number of synapses. Fold increase is calculated based on the number of synapses formed by RGCs cultured alone (mean synapse number for RGC-alone condition, 3.0 ± 0.67). Astrocyte feeding layers or hevin all significantly increased the number of colocalized synaptic puncta versus RGCs cultured alone (*$P <$ 0.05; n = 20 cells per condition; error bars indicate SEM). (*E*) Quantification of the effects of different concentrations of hevin on the number of synapses formed by RGCs in culture. Fold increase is calculated based on the number of synapses formed by RGCs cultured alone (mean synapse number for RGC-alone condition, 0.933 ± 0.27; *$P <$ 0.05; n = 20 cells per condition; error bars indicate SEM).

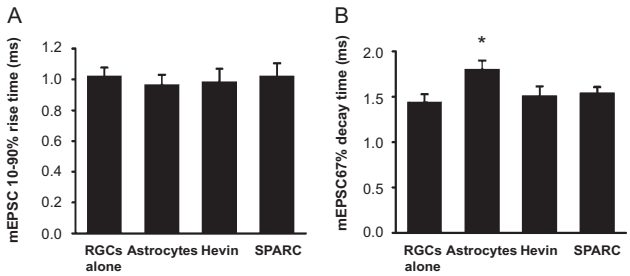

Fig. S2. Hevin induces formation of postsynaptically silent synapses (*A*). Quantification of the 10% to 90% rise time of mEPSCs from RGCs cultured alone (control), with astrocytes, with 30 nM Hevin, or with 100 nM SPARC ($n = 12$ cells per condition; error bars indicate SEM). (*B*) Quantification of the 67% decay time of mEPSCs from RGCs cultured alone (control), with astrocytes, with 30 nM Hevin, or with 100 nM SPARC. (*$P < 0.005$; $n = 12$ cells per condition; error bars indicate SEM).

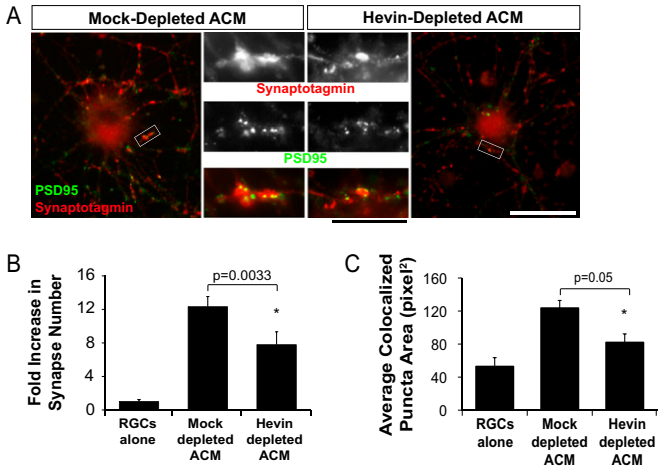

Fig. S3. Depletion of hevin from ACM reduces synapse number and synaptic size. (*A*) Hevin depletion led to a decrease in synapse number and synaptic size. High-magnification images of RGC synapses are marked by white rectangles (*Middle*) stained with presynaptic vesicular marker synaptotagmin (red) and postsynaptic marker PSD95 (green). Colocalized puncta in merged images represent synapses. (Scale bars: white, 30 μm; black, 10 μm.) (*B*) Quantification of colocalized synaptic puncta showed that RGCs cultured with hevin-depleted ACM formed 40% fewer synapses compared with RGCs treated with mock-depleted ACM. Fold increase is calculated based on the number of synapses formed by RGCs cultured alone (mean synapse number for RGC-alone condition, 1.40 ± 0.37; *$P = 0.0033$; $n = 20$ cells per condition; error bars indicate SEM). (*C*) Quantification of average synapse size (average size of colocalized puncta) throughout the conditions showed that hevin depletion leads to a significant decrease in the size of the synapses formed in response to ACM (*$P = 0.05$; $n = 20$ cells per condition; error bars indicate SEM).

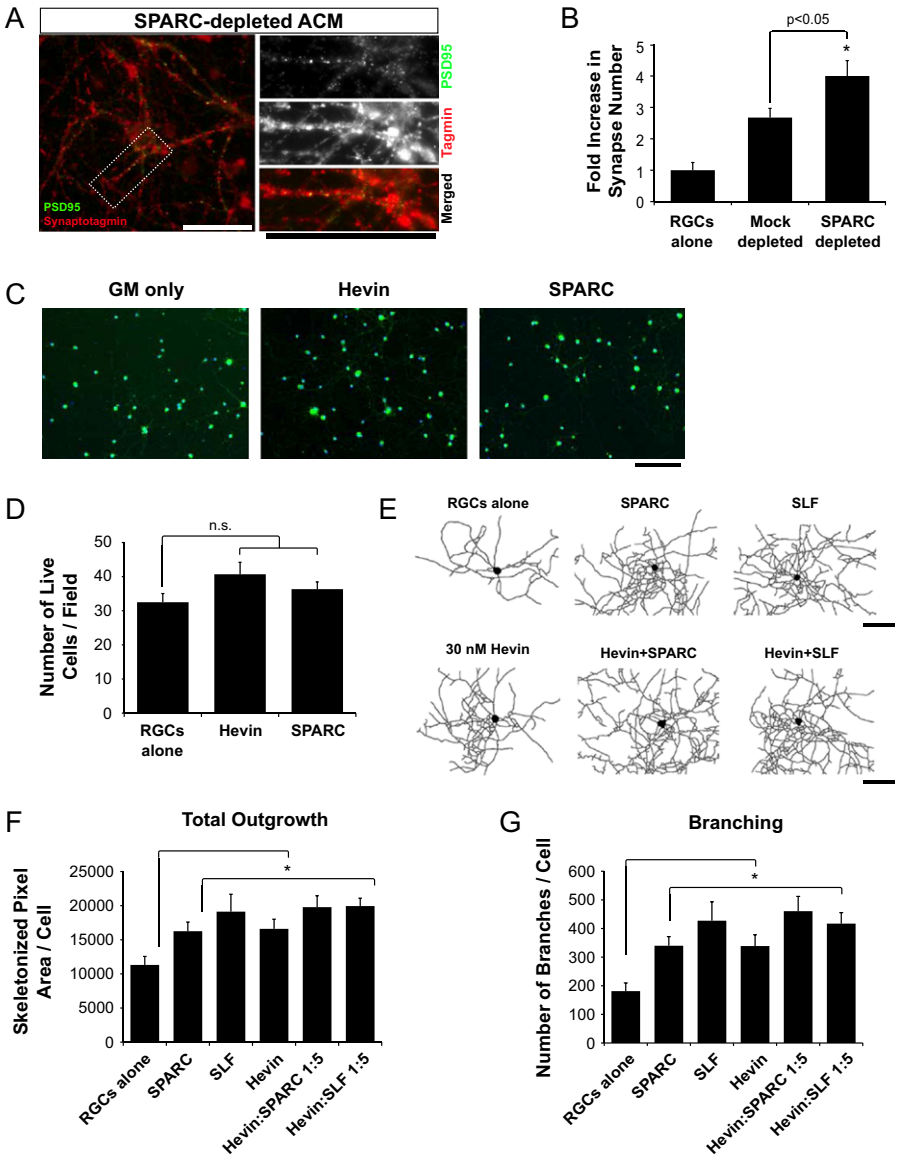

Fig. S4. SPARC antagonizes the synaptogenic activity of hevin. (*A*) Synapse formation is enhanced when RGCs in culture are treated with SPARC-depleted ACM. Immunostaining by presynaptic vesicular marker synaptotagmin (red) and postsynaptic marker PSD95 (green) show increased synapse number and increased innervations of the cell body and proximal dendrites by the synaptic specializations. (Scale bar: 30 μm.) (*B*) Quantification of synapse number in RGCs cultured in the presence of SPARC-depleted rat ACM versus mock-depleted rat ACM. In the presence of SPARC-depleted ACM, synapse number per RGC increases 30% compared with mock-depleted ACM (mean synapse number for RGC-alone condition, 1.40 ± 0.37; $^*P < 0.05$; $n = 15$ cells per condition; error bars indicate SEM). (*C*) Representative images of calcein-AM green–positive live 10 DIV RGCs cultured in growth media (GM) alone or with 30 nM Hevin or 150 nM SPARC. (Scale bar: 100 μm.) (*D*) Quantification of live cells (calcein green-positive) per field (*P* values not significant; $n = 15$ fields per condition, i.e., five fields per replica and three replicas per condition). (*E*) Representative skeletonized traces of RGCs transfected with td-tomato fluorescent protein that were cultured in growth media alone or treated with SPARC (150 nM), hevin (30 nM), hevin plus SPARC (30 nM and 150 nM, respectively), SLF (150 nM), or hevin plus SFL (30 nM and 150 nM, respectively). Hevin, SPARC, and SLF alone or in combination promoted neurite outgrowth. (Scale bar: 100 μm.) Quantification of total outgrowth (*F*) and number of branch points (*G*) per cell under conditions listed in *E*. The analysis was done by using 12-bit monochrome images of td-tomato–transfected RGCs by using the Metamorph Neurite Outgrowth Analysis option ($^*P < 0.001$; $n > 20$ cells per condition; error bars indicate SEM).

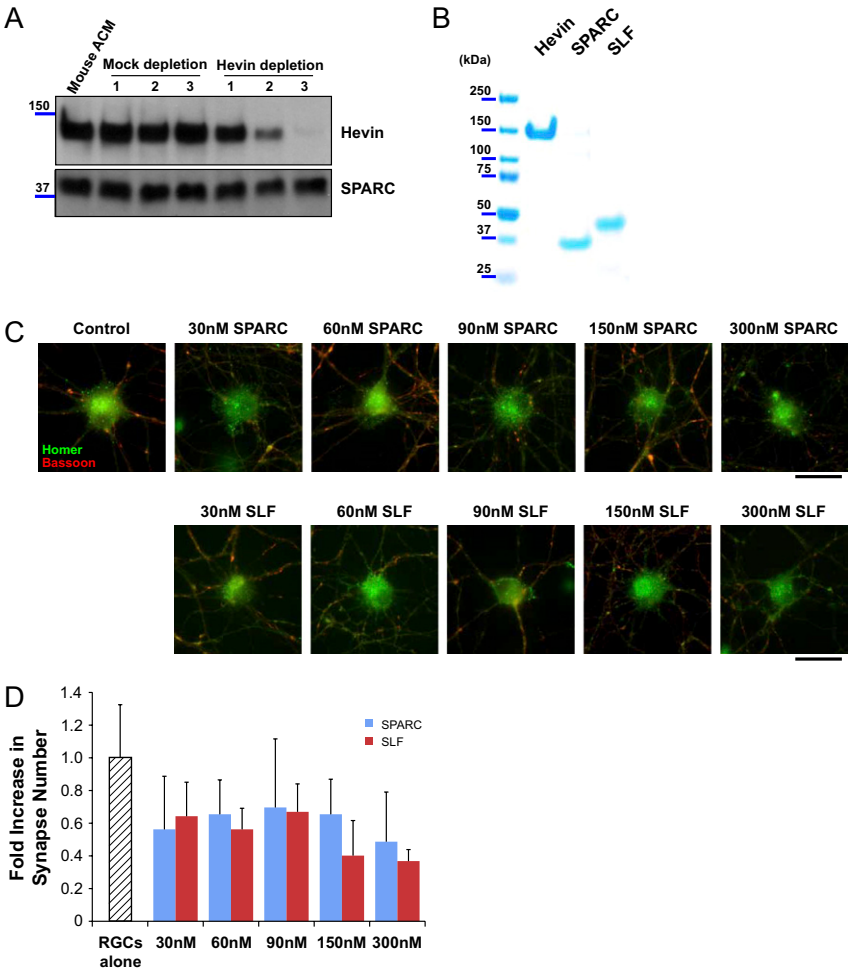

Fig. S5. SPARC and SLF are not synaptogenic. (*A*) Western blot analysis of hevin immunodepletion samples with anti-hevin or anti-SPARC antibodies. Hevin and SPARC do not interact in the ACM because SPARC levels in ACM do not change with hevin immunodepletion. (*B*) Coomassie blue staining of hevin, SPARC, and SLF proteins purified by Ni-chelating chromatography. (*C*) Representative images of RGCs that were cultured alone or with increasing doses of SPARC or SLF (30, 60, 90, 150, 300 nM) and stained with presynaptic marker bassoon (red) and postsynaptic marker homer (green). SPARC or SLF treatments did not induce colocalized synaptic puncta in RGCs. (Scale bars: 30 μm.) (*D*) Quantification of the fold changes in colocalized synaptic puncta number per cell for RGCs cultured alone or with increasing doses of SPARC or SLF (30, 60, 90, 150, 300 nM). Fold increase is calculated based on the number of synapses formed by RGCs cultured alone (mean synapse number for RGC-alone conditions, 3.73 ± 1.21). Synaptic density indicates the number of synapses per 100 μm neurite (*P* values not significant; *n* = 15 cells per condition; error bars indicate SEM).

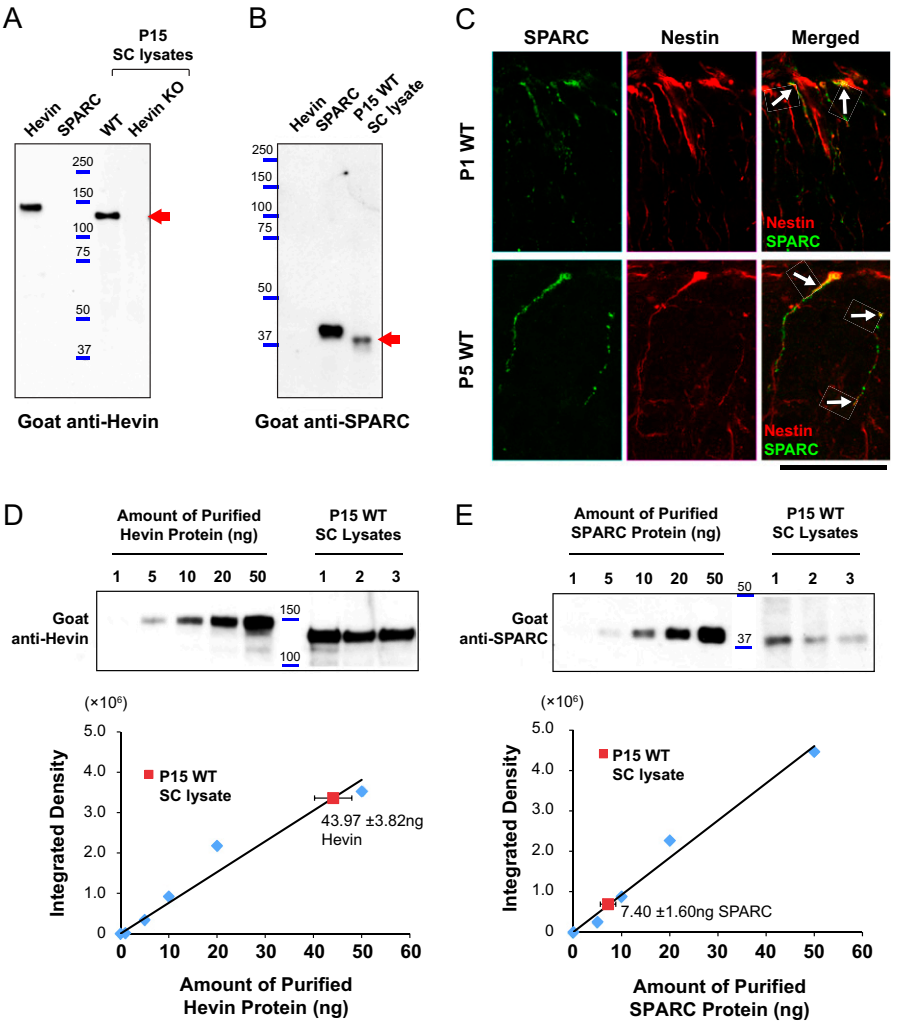

Fig. S6. Characterization of goat anti-Hevin and goat anti-SPARC antibodies used for Western blot analysis shown in Fig. 6. (*A*) Western blot analysis of 75 ng pure hevin, 75 ng pure SPARC, and SC lysates from P15 WT and hevin-null (KO) mice with goat anti-hevin polyclonal antibody (R&D Systems). This antibody specifically recognizes a 130-kDa band in WT lysate corresponding to hevin protein that is absent from KO lysate. Moreover, this antibody does not cross-react with purified SPARC (lane 2). The recombinant hevin runs at a slightly higher molecular weight than the endogenous hevin protein as a result of additional protein purification and identification tags (Fig. 5*A*). (*B*) Western blot analysis of 75 ng pure hevin or 75 ng pure SPARC and SC lysate from P15 WT mice by using goat anti-SPARC polyclonal antibody (R&D Systems). This antibody specifically recognizes an approximately 43-kDa band corresponding to SPARC in WT SC lysate and does not cross-react with purified hevin. The recombinant SPARC runs at a slightly higher molecular weight than the endogenous SPARC protein as a result of an additional 6-histidine tag (Fig. 5*A*). (*C*) SPARC is expressed by radial glia in the SC at P1 and P5. Sagittal sections of SC from P1 or P5 mouse brains were stained for a radial glial marker, nestin (red), and SPARC (green). SPARC staining localizes along the length of radial glia (white arrows). (Scale bar: 50 μm.) Comparative analyses of hevin (*D*) and SPARC (*E*) protein levels in P15 mouse SC lysates by Western blotting. Purified hevin or SPARC proteins at different amounts were analyzed by Western blotting along side 15 μg of SC lysates from three different P15 mouse SCs. The signal intensities for each band (i.e., integrated density) were determined by ImageJ. Integrated densities were plotted against pure protein amounts. Linear curves were fitted and used to calculate the mean hevin (43.97 ± 3.82 ng per 15 μg lysate) and SPARC (7.40 ± 1.60 ng per 15 μg) amounts in the P15 SC lysates.

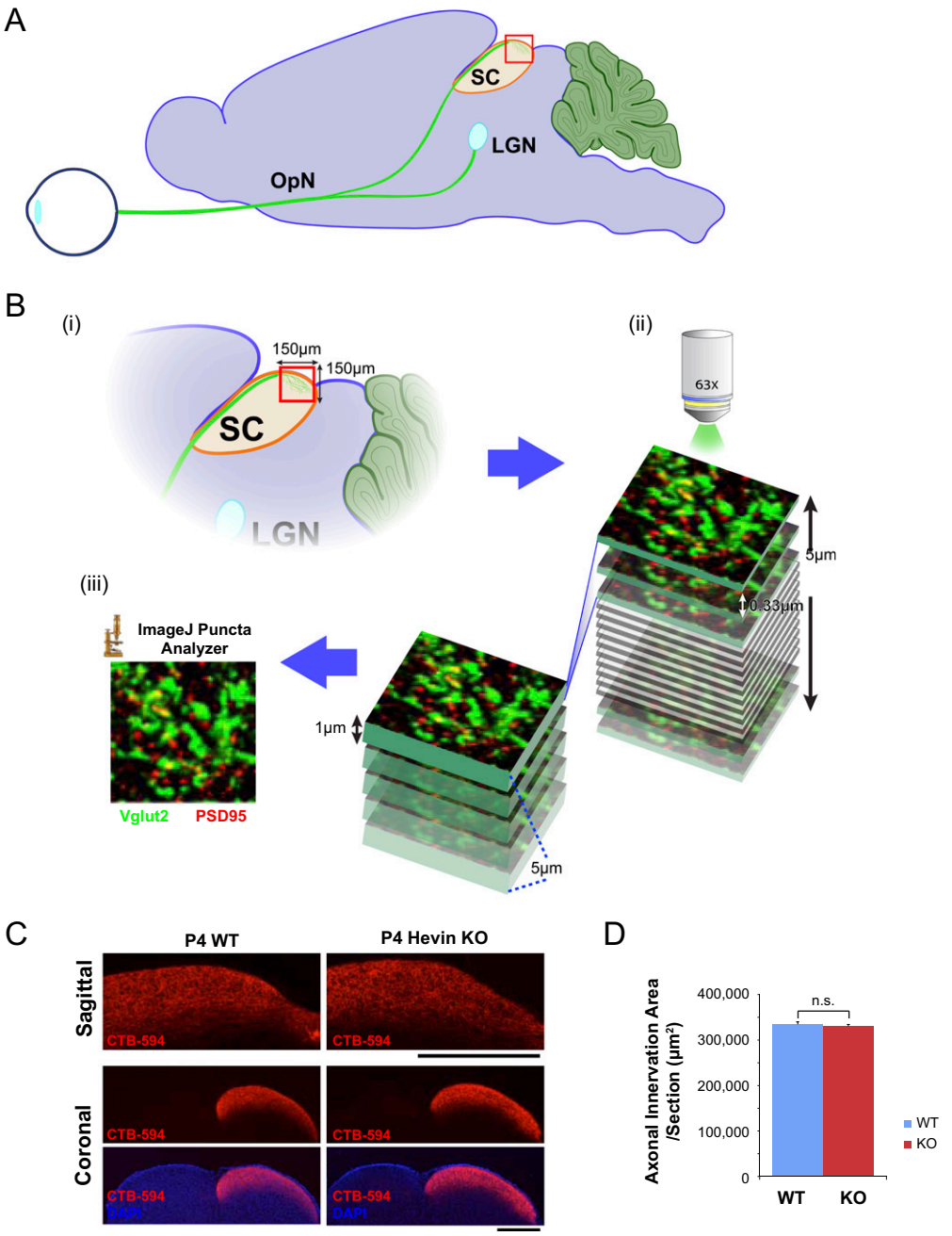

Fig. S7. Schematic presentation of quantification of colocalized synaptic puncta by IHC and confocal microscopy. (*A*) RGC axons project to their synaptic targets in the brain, including lateral geniculate nucleus (LGN) and SC. (*B*) For analysis of synapse number and size, we stained sagittal mouse brain sections and determined synaptic density within an area of 150 × 150 μm of the SC encompassing the zone where RGC axons form synapses (*i*). By using laser scanning confocal microscopy, retinocollicular synapses stained with VGlut2 and PSD95 were imaged. Z-stacks of 15 images with 0.33-μm steps corresponding to a 5-μm depth were acquired for each brain section (*ii*). Three independent brain sections were scanned per animal, and four animals per age per genotype were analyzed. (*iii*) Maximal projections were made for each of the three consequent optical sections (five images per section). These images were quantified by using ImageJ with the puncta analyzer plug-in, which determines the number and size of colocalized puncta. (*C*) Unilateral eye injections of CTβ (CTB-594) to trace RGC axonal terminals at the SC showed that RGC axons in Hevin-KO mice form normal longitudinal innervations (*Upper*, sagittal) and midline targeting (*Lower*, coronal). (Scale bars: 500 μm.) (*D*) Quantification of the CTB-594–positive RGC axonal innervation areas in WT and Hevin-KO SC ($n = 4$ animals, n.s., not significant; error bars indicate SEM).

Table S1. Study details in WT and hevin-KO mice

Detail	WT	Hevin KO
Animals used	3	3
High-magnification images analyzed	432	449
Total area analyzed, μm^2 (cell bodies excluded)	4,210	4,326
Total asymmetric synapses analyzed	431	289
Symmetric synapses	149	179
Asymmetric multiple synapses	53	30

Table S2. *Hevin*-null mice have morphological defects in asymmetric synapses at the SC

	Mean ± SEM			
Characteristic	WT	Hevin KO	Difference: KO vs. WT, %	*P* value
Synaptic density/100 μm^2 (asymmetric)	10.49 ± 0.82	7.13 ± 0.69	−32.1	0.005
Synaptic density/100 μm^2 (symmetric)	3.67 ± 0.61	4.66 ± 0.88	NS	0.19
Synaptic density/100 μm^2 (asymmetric multiple)	1.25 ± 0.11	0.75 ± 0.10	−40.0	0.003
Asymmetric/symmetric ratio (synaptic density/100 μm^2)	2.61 ± 0.20	1.57 ± 0.19	−39.6	0.002
Morphological parameters of asymmetric synapses				
Morphology				
PSD length, nm	197.0 ± 3.7	192.6 ± 5.0	NS	0.22
PSD thickness, nm	37.49 ± 0.88	22.93 ± 0.88	−38.9	5.4×10^{-19}
Synaptic cleft distance, nm	8.57 ± 0.51	12.12 ± 0.62	+41.5	0.0003
Presynaptic area, μm^2	0.83 ± 0.03	0.52 ± 0.03	−37.1	2.0×10^{-11}
Presynaptic perimeter, μm	4.75 ± 0.12	3.53 ± 0.12	−25.6	2.8×10^{-10}
SV				
Synaptic vesicles/synapse/section	59.3 ± 2.8	28.4 ± 1.5	−52.2	1.9×10^{-18}
Docked vesicles/synapse/section	6.7 ± 0.3	4.6 ± 0.2	−31.0	1.0×10^{-19}

NS, not significant.